



Ultrasound neuromodulation of cultured hippocampal neurons

Seoyoung Hwang^{1,4} · Sang Beom Jun^{1,2,3}

Received: 25 May 2023 / Revised: 24 July 2023 / Accepted: 14 August 2023 / Published online: 2 September 2023
© Korean Society of Medical and Biological Engineering 2023

Abstract

Ultrasound is becoming an emerging and promising method for neuromodulation due to its advantage of noninvasiveness and its high spatial resolution. However, the underlying principles of ultrasound neuromodulation have not yet been elucidated. We have herein developed a new in vitro setup to study the ultrasonic neuromodulation, and examined various parameters of ultrasound to verify the effective conditions to evoke the neural activity. Neurons were stimulated with 0.5 MHz center frequency ultrasound, and the action potentials were recorded from rat hippocampal neural cells cultured on microelectrode arrays. As the intensity of ultrasound increased, the neuronal activity also increased. There was a notable and significant increase in both the spike rate and the number of bursts at 50% duty cycle, 1 kHz pulse repetition frequency, and the acoustic intensities of 7.6 W/cm² and 3.8 W/cm² in terms of spatial-peak pulse-average intensity and spatial-peak temporal-average intensity, respectively. In addition, the impact of ultrasonic neuromodulation was assessed in the presence of a gamma-aminobutyric acid A (GABA_A) receptor antagonist to exclude the effect of activated inhibitory neurons. Interestingly, it is noteworthy that the predominant neuromodulatory effects of ultrasound disappeared when the GABA_A blocker was introduced, suggesting the potential of ultrasonic stimulation specifically targeting inhibitory neurons. The experimental setup proposed herein could serve as a useful tool for the clarification of the mechanisms underlying the electrophysiological effects of ultrasound.

Keywords Ultrasound · Neuromodulation · Multielectrode arrays · Hippocampal cell culture

1 Introduction

Neuromodulation is a technique that activates or inhibits a part of the nervous system with various modalities. As nerve cells transmit information through electrochemical signals, neuromodulation techniques have been extensively

used in neuroscientific studies and clinical applications [1]. The most common neuromodulation method by applying external stimuli is electric stimulation. An electrical current or voltage from an electrode directly connected to a nerve cell can change its membrane potential. In recent years, neuromodulation approaches using optogenetics have been widely studied in neuroscience studies [2]. Optogenetics is a neuromodulation technique that uses light, and it enables it to selectively excite or inhibit neurons by manipulating nerve cells genetically to react to a specific light [3–5]. However, these electrical neuromodulations require invasive surgery, and in the case of optogenetics, they entail the expression of exogenous proteins and the implantation of a light source [2, 6].

To resolve this drawback, noninvasive methods such as transcranial magnetic stimulation (TMS) and transcranial direct current stimulation (tDCS) have been utilized more broadly for the treatment of neurological disorders [7–9]. However, both TMS and tDCS have limitations when it comes to transmitting with the low spatial resolution to the target brain regions of interest [10]. Ultrasound is an

✉ Sang Beom Jun
juns@ewha.ac.kr
Seoyoung Hwang
seoyoung711@gmail.com

¹ Department of Electronic and Electrical Engineering, Ewha Womans University, 52 Ewhayeodae-gil, Seodaemun-gu, Seoul 03760, Republic of Korea
² Graduate Program in Smart Factory, Ewha Womans University, Seoul, Republic of Korea
³ Department of Brain and Cognitive Sciences, Ewha Womans University, Seoul, Republic of Korea
⁴ Seoul National University Hospital Biomedical Research Institute, Seoul National University Hospital, Seoul, Republic of Korea

emerging and promising method of inducing neuromodulation due to its advantage of noninvasiveness and its high spatial resolution. Ultrasound is an acoustic sound pressure wave in a frequency range that is above the human hearing levels (generally, > 20 kHz) and exerts no electrochemical side effects. In addition, it can be emitted noninvasively at various intensities with a high spatial resolution focus up to a few millimeters or submillimeters.

When compared with other ultrasonic applications of therapeutic ablations or medical imaging, ultrasound was recently commenced as a neuromodulation approach, and its underlying mechanism is still being studied. For the induction of thermal ablation or the mechanical fractionation of soft tissues, high-intensity ultrasound (known as high-intensity focused ultrasound (HIFU)) has been used. HIFU typically requires over 1 kW/cm², and the power levels equal to or less than 1 W/cm² are considered of low-intensity without induction of mechanical bioeffects [2, 6, 11].

In 2008, Khraiche showed that the frequency of action potentials of rat hippocampal cells was increased after applying ultrasound waves of 7.75 MHz for one min to neurons cultured on microelectrode arrays (MEA) [12]. Tyler group observed an increasing activity of the rodent hippocampal slices through fluorescence imaging [13]. In 2009, Muratore figured out the increase of the local field potential by irradiating ultrasound for 1 ms on brain slices [14]. In 2011, Tufai described the general protocol for the *in vivo* use of low-intensity focused ultrasound brain stimulation in the motor cortex of mice [15]. More recently, ultrasound neuromodulation experiments with various stimulating conditions were performed. However, the precise parameters for the induction of effective neuromodulation were still unclarified. Pulsed ultrasound was sonicated into the anesthetized rodent motor brain area while observing the motor responses [16]. Similarly, pulsed ultrasound was found to modify the activity of the sensory receptors on the skin [17]. Although the various variables for ultrasound-induced neuromodulation were examined using a diverse animal model, there are insufficient standards for the assessment of the ultrasound effects.

In this study, we have developed a new experimental setup with planar-type MEAs to directly investigate effect of ultrasonic neuromodulation on cultured neurons. Then, we have examined the ultrasound-induced changes of the neuronal activity in the primary hippocampal neurons cultured on the MEA with various ultrasonic parameters including intensity, duty cycle, sonication duration, and pulse repetition frequency. In addition, to investigate the role of inhibitory neurons under ultrasound exposure, the ultrasound-induced neural activity was analyzed in the presence of inhibitory neuron blocker.

2 Materials and methods

2.1 Ultrasound system

A custom-made water-immersion 10 × 10-mm square ultrasound transducer (TKS Corp., Busan, Republic of Korea) was used for experiments. Electrical pulses with the fundamental frequency of 0.5 MHz were generated using a function generator (33220A Function; Agilent Technologies Inc., CA, USA) and were amplified using a radio frequency amplifier (240L; Electronics & Innovation, Rochester, NY). Ultrasound signals were measured using a calibrated hydrophone (HNR-0500; ONDA Corporation, Sunnyvale, CA) with an oscilloscope (DSO9102A; Agilent Technologies, Inc.). The mechanical index (MI) and acoustic intensity were calculated using equations as previously modified [15].

MI was defined as follows:

$$MI = \frac{P_r}{\sqrt{f}},$$

where P_r is the peak rarefactional pressure and f is the fundamental frequency. And, to compute acoustic intensity, the pulse intensity integral (PII) was defined as follows:

$$PII = \int \frac{P^2(t)}{Z_0} dt,$$

where P is the peak pressure and Z_0 is the acoustic impedance defined as ρc (ρ is the density of the medium (1,028 kg/m³) and c is the speed of sound in the medium (1,515 m/s)). The spatial-peak pulse-average intensity (I_{SPPA}) was estimated by dividing PII with the pulse duration, and the spatial-peak temporal-average intensity (I_{SPTA}) was calculated by multiplying the duty cycle with I_{SPPA} . The duty cycle is the percentage of sonication described as the product of the pulse duration (PD) (in ms) and pulse repetition frequency (PRF; in kHz) is shown in Fig. 1a [16]. We positioned the ultrasound transducer and hydrophone to measured acoustic intensity in a similar condition of the neuromodulation experiment with cultured neurons as shown in Fig. 1b. In order to locate the hydrophone at the MEA surface, we modified a PCB-based MEA (MEA60 100 Pt Model, Ayanda Biosystems, Lausanne, Switzerland), which has a glass microelectrode part attached with the PCB substrate. The glass microelectrode was detached and a sheet of Parafilm (Sigma-Aldrich Inc., St. Louis, USA), was attached. Then the hydrophone was located at the surface through the film. To ensure a constant pressure, every experiment was conducted at a 3-mm distance between the transducer and the surface of MESs.

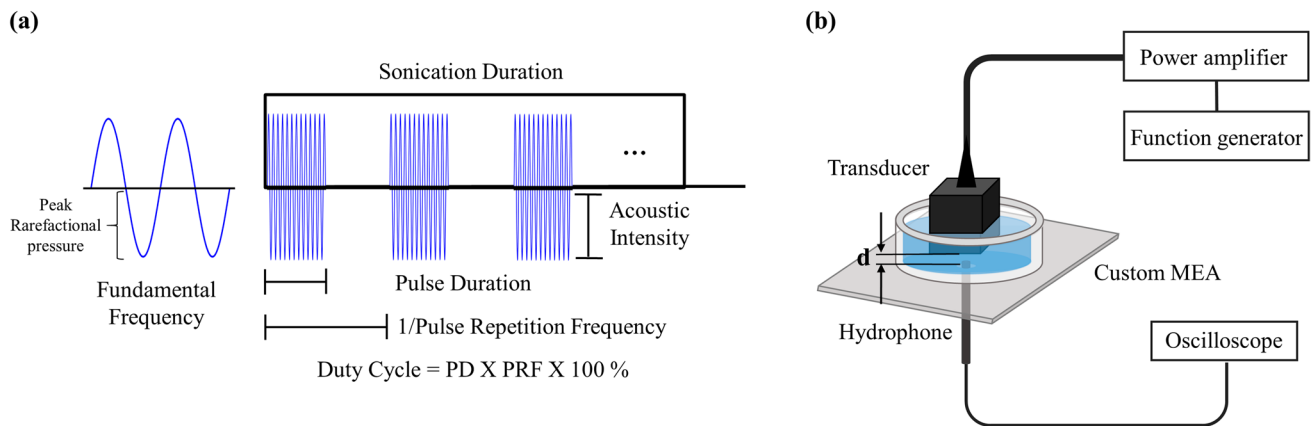


Fig. 1 The definitions of ultrasound parameters and the experimental setup for the ultrasound intensity measurement. **a** 0.5 MHz fundamental frequency was applied into the transducer with a factor of acoustic intensity, pulse duration, PRF, and sonication duration. Duty

cycle is determined as a ratio of pulse duration in a single repetition period. **b** The hydrophone was set at the bottom of the MEA, and the transducer was located over the MEA in the culture medium

2.2 Primary cell culture

Primary hippocampal neurons were prepared from embryonic (E17–18) Sprague Dawley rats according to a previously modified protocol [18]. Briefly, the embryos' hippocampi were dissected in cold Hanks' balanced salt solution (Gibco®, Carlsbad, USA) and were then incubated in 0.5% trypsin–EDTA (Gibco®) for 15 min. After the digestion of trypsin, tissues were rinsed five times in phosphate-buffered saline (Gibco®) and were triturated using a 1-mL pipette tip. Neurons were seeded at a density of 1,800 cells/mm² on microelectrode arrays (MEA; Multichannel System GmbH, Reutlingen Germany). Cells were incubated in Dulbecco's Modified Eagle Medium (Gibco®) supplemented with 10% horse serum (Gibco®) and 1% antibiotic–antimycotic solution (Gibco®) as a plating medium. After 1 h, the plating medium was replaced by a culture medium consisting of serum-free neurobasal medium (Gibco®) supplemented with 2% B27 (Gibco®) and 1% GlutaMAX (Gibco®), and the cells were maintained at 37 °C in a 5% CO₂ and 95% air humidified atmosphere. One week later, half of the culture medium was changed twice a week. Ultrasonic neuromodulation experiments were performed after 14 days in vitro (DIV), when the cells are believed to have become mature neurons [19].

2.3 Recording system

We used the planar-type MEA that had 60 electrodes with a 200-μm spacing and a 30-μm site diameter. The electrode material was titanium nitride on the indium-tin-oxide conductor lines, and the insulation material was silicon nitride. Before the experiment, MEA were submitted to a cleaning procedure: they were soaked in Terg-A-zyme detergent

(Sigma-Aldrich Inc.) for at least 1 h, were washed thoroughly with distilled water, autoclaved and sonicated, and UV-sterilized in dry conditions. The MEAs were finally coated with poly-D-lysine (Sigma-Aldrich Inc.) for at least 3 h to promote cell adhesion.

Neural activities were recorded using a data acquisition card (Multichannel System GmbH) with 1,100 gain amplification with 25 kHz sampling. The temperature of culture medium was monitored and maintained at 37 °C using a PH01 temperature controller (Multichannel System GmbH). The recorded data were collected and analyzed using the MC_Rack software (Multichannel System GmbH). Using a high-pass filter with a cutoff frequency of 200 Hz, field potentials were eliminated. The threshold for spike detection was set at five times the standard deviation of the background noise [20]. Bursts were defined using the Max Interval algorithm [21]. We set the maximal interval between spikes to start burst at 10 ms, the maximal interval between spikes to end burst at 100 ms, the minimal interval between bursts at 210 ms, the minimal duration of a burst at 50 ms, and the minimal number of spikes within bursts at five. Images were visualized using an inverted microscope (IX71; Olympus, Tokyo, Japan) and were collected using a complementary metal–oxide semiconductor (CMOS) camera (Zyla 5.5 sCMOS; Andor, UK).

2.4 Experimental protocol and parameters

Prior to the experiment, the culture medium was replaced by artificial cerebrospinal fluid (aCSF) of the following composition (in mM): 124 NaCl, 4.5 KCl, 1.2 NaH₂PO₄, 26 NaHCO₃, 1 MgCl₂, 2 CaCl₂, and 10 glucose with 5% CO₂ bubbling. Cells were kept for over 15 min in the incubator for stabilization. To identify the effective conditions,

different sonication parameters were tested (Fig. 1b). We examined five levels of acoustic intensity (levels 1–5), three duty cycles (10, 50, and 90%), three sonication durations (20, 60, and 120 s), and five PRFs (10, 100, 500, 1000, and 2000 Hz). Before ultrasound stimulation, the neuronal activities were recorded for one min as a baseline condition. Then, ultrasonic stimulation with each parameter was applied for 20 s except the experiments with different sonication durations. After the stimulation, action potentials were recorded for one min and the activities were analyzed. Same electrodes of MEAs were used for neural recording of baseline and the neural activity induced by the sonication. 3–6 MEAs were used for analysis for each parameter, and statistical analyses were performed using APs detected from an average of 18 or more electrodes per MEA.

2.5 Drug treatment

Bicuculline (Sigma-Aldrich, Inc.), a gamma-aminobutyric acid A receptor ($GABA_A$) antagonist was administered to block the inhibitory neuronal activity in the cultured neurons [20, 22]. Bicuculline was dissolved in dimethyl sulfoxide (DMSO; Sigma-Aldrich, Inc.), and concentrations of 25 μM were administered to neurons cultured on the MEAs [23–25]. At the presence of bicuculline, the same experiments for ultrasound neuromodulation were performed.

2.6 Statistical analysis

A raster plot was constructed using the NeuroExplorer software (Nex Technologies, MA, USA). Data were presented as mean \pm standard mean error (SEM). Statistical significance was analyzed using the one-way repeated measurement ANOVA, followed by a Bonferroni *post-hoc* test in GraphPad Prism 5.0 (GraphPad software, San Diego, USA). Values of P that were less than 0.05 were considered statistically significant.

3 Results

3.1 Performance of ultrasound

Hippocampal neurons were cultured on MEA at a density of 1,800 cells/ mm^2 and to maintain a distance that would ensure a constant pressure, 3D-printed plastic mold was introduced so that every experiment would be conducted precisely at 3 mm distance from the cell (Fig. 2). At 3-mm distance, the pressures were measured as 0.06, 0.24, 0.34, 0.49, and 0.78 MPa for the level 1 to 5 (Fig. 3).

Table 1 presents the mechanical indices and the acoustic intensity of each level. I_{SPPA} value was equal to the value when I_{SPTA} duty cycle was 100%. Acoustic intensity

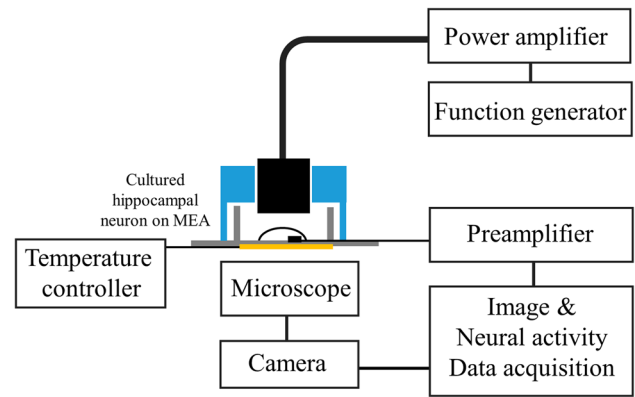


Fig. 2 Diagram of the experimental setting. Hippocampal neurons were cultured on MEA and were ultrasound-irradiated through a transducer set on the MEA with a 3D mold connected to a power amplifier and a function generator. The neuronal signal was recorded through the electrodes of the MEA

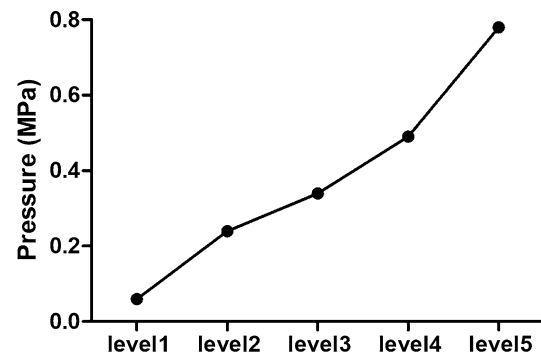


Fig. 3 Graph of the ultrasound pressure of the transducer at a distance of 3 mm

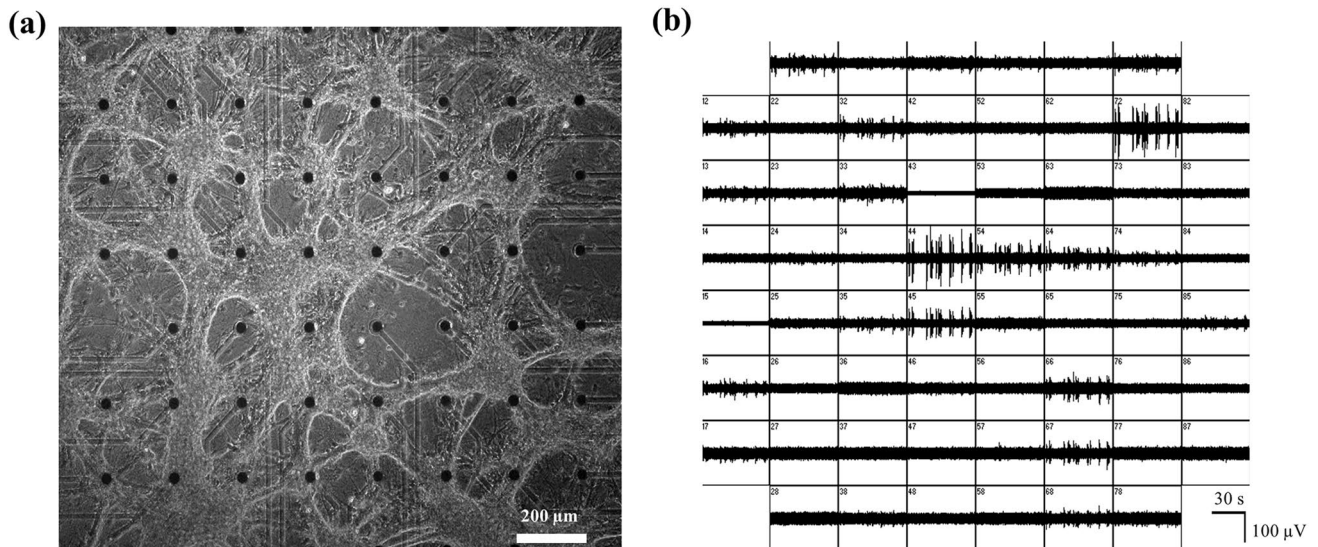
increased when the level and duty cycle were increased. According to the Food and Drug Administration (FDA) guideline, the mechanical index (MI) value should not exceed 1.9 to avoid inertial cavitation in the tissue [26]. In this experiment, the highest value of MI used was 1.1, and therefore, our experiments were performed within the safety range.

3.2 Effects of different ultrasound acoustic intensities

On DIV 14, the ultrasound stimulation was applied to the neurons cultured on the MEAs. The action potentials (APs) of the hippocampal neurons cultured on MEAs were recorded (Fig. 4a and b). APs and their bursts were analyzed for each ultrasound acoustic intensity level. Other parameters were fixed at a duty cycle of 50%, a sonication duration of 20 s, and a PRF of 1 kHz. A raster plot of 1-min duration after the ultrasound stimulation

Table 1 Characteristics of the acoustic intensity of the ultrasound

	Output (V)	Pressure (MPa)	Mechanical index	I_{SPPA} (W/cm^2) (I_{SPTA} , DC = 100%)	I_{SPTA} (W/cm^2)		
					DC = 10%	DC = 50%	DC = 90%
Level 1	44.4	0.06	0.09	0.11	0.01	0.06	0.10
Level 2	176.8	0.24	0.34	1.45	0.15	0.72	1.30
Level 3	250.6	0.34	0.14	3.26	0.33	1.63	2.93
Level 4	371.9	0.49	0.69	7.66	0.77	3.83	6.84
Level 5	574.1	0.78	1.10	17.38	1.74	8.70	15.64

**Fig. 4** Hippocampal neurons on MEA. **a** Phase-contrast microscope image of the hippocampal cells at DIV 14 and at a density of 1,800 cells/ mm^2 . **b** The neural activity of a hippocampal cells on MEA

(Fig. 5a). Spike frequency and number of bursts were normalized by the data from baseline conditions (Fig. 5b and c). When compared with the baseline, the spike rate was found increased as acoustic intensity increased and Bonferroni *post-hoc* analysis revealed the statistical significance at levels 4 and 5 (Fig. 5b; spike rate: 0.64 ± 0.13 Hz at baseline, 0.51 ± 0.1 Hz at level 1, 1.00 ± 0.26 Hz at level 2, 1.29 ± 0.38 Hz at level 3, 1.60 ± 0.52 Hz at level 4, and 1.88 ± 0.55 Hz at level 5). The number of bursts was also increased with the statistical significance at levels 3, and 5 (Fig. 5c; 1.07 ± 0.35 at baseline, 0.91 ± 0.27 at level 1, 2.03 ± 0.51 at level 2, 3.03 ± 0.86 at level 3, 3.0 ± 0.94 at level 4 and 3.94 ± 1.23 at level 5) The burst duration was also analyzed (Fig. 5d; 25.81 ± 5.06 ms at baseline, 29.83 ± 5.92 ms at level 1, 46.75 ± 10.16 ms at level 2, 41.29 ± 9.82 ms at level 3, 44.66 ± 11.76 ms at level 4 and 61.41 ± 10.55 ms at level 5). There was only one significant change in the burst duration at level 5.

3.3 Effects of different ultrasound duty cycles, sonication durations, and PRFs

The mean spike rates and the number of bursts were analyzed for different duty cycles, sonication durations, and PRFs of ultrasound. The response patterns for the duty cycle are presented in Figs. 6a and d. When the duty cycle parameter experiment was carried out, other factors were fixed at an acoustic intensity of level 2, 20-s sonication duration, and 1 kHz PRF. The frequency of the spikes and the number of bursts were normalized by baseline (Fig. 6a; spike rate: 0.15 ± 0.03 Hz at baseline, 0.18 ± 0.04 Hz at 10%, 0.24 ± 0.05 Hz at 50%, and 0.2 ± 0.04 Hz at 90%, Fig. 6d; number of bursts: 0.1 ± 0.04 at baseline, 0.23 ± 0.08 at 10%, 0.36 ± 0.12 at 50% and 0.22 ± 0.05 at 90%). The highest increase was observed in both the spike frequency and the number of bursts when the stimulation with a 50% duty cycle was applied.

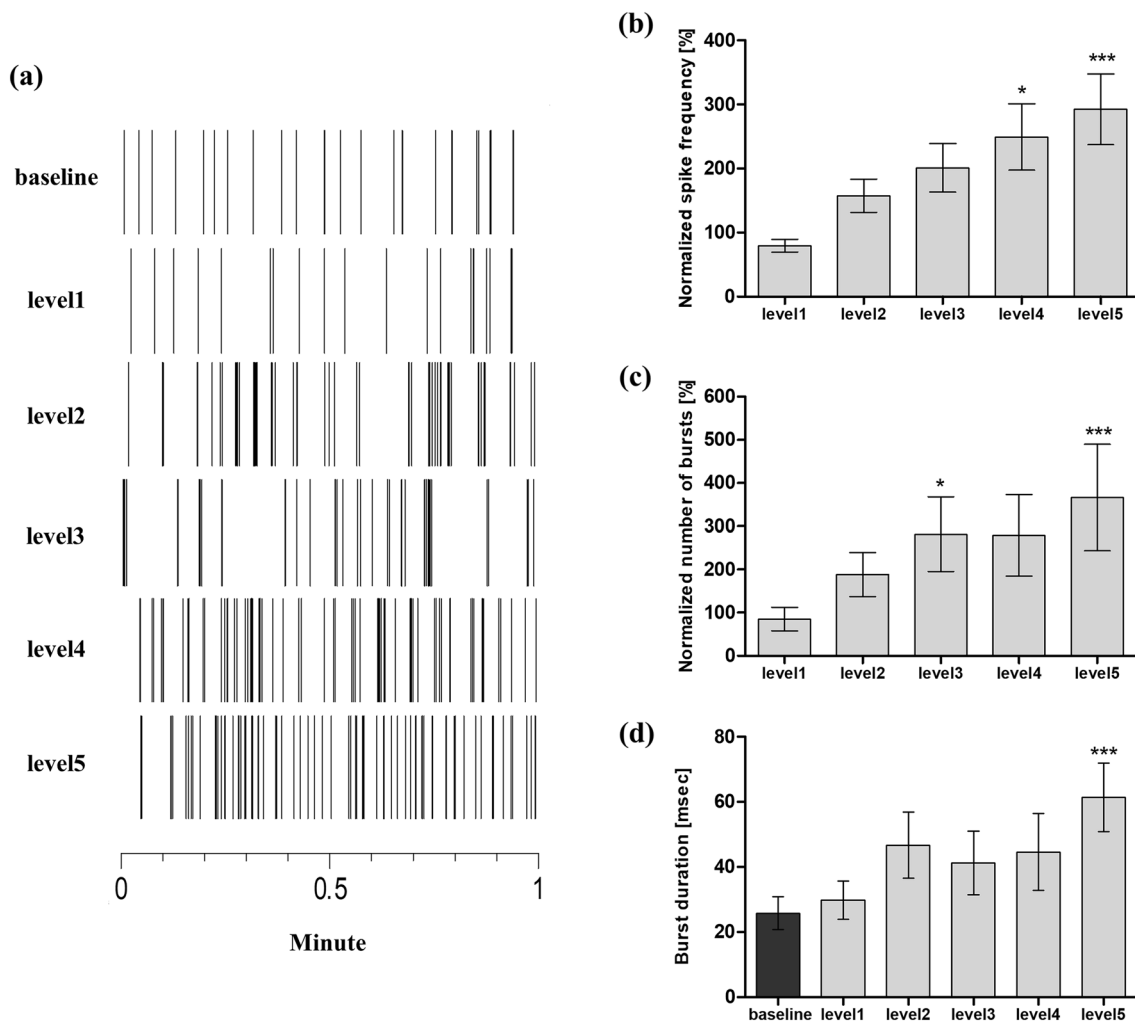


Fig. 5 Characteristics of the neuronal response (given as mean \pm SEM) to different acoustic intensity levels. **a** Raster plot of neural spikes recorded on MEA. **b** Normalized spike frequency **c** Normalized number of bursts **d** Mean burst duration in response

The effects of different sonication durations are presented in Fig. 6b and e. The other ultrasound parameters were fixed at an acoustic intensity of level 2, 50% duty cycle, and 1 kHz PRF. The frequency of the spikes and the number of bursts were normalized by baseline (Fig. 6b; spike rate: 0.3 ± 0.07 Hz at baseline, 0.28 ± 0.06 Hz at 20 s, 0.38 ± 0.1 Hz at 60 s, and 0.53 ± 0.24 Hz at 120 s, Fig. 6e; number of bursts: 0.53 ± 0.18 at baseline, 0.43 ± 0.13 at 20 s, 0.57 ± 0.21 at 60 s and 0.69 ± 0.24 at 120 s). In the case of the sonication duration, no significant difference was identified when compared with baseline. However, the longer the sonication lasts, the larger the variation of the cell activity becomes. A similar phenomenon was observed in the case of the burst number.

The changes in activity in response to the variations of the PRF factor were analyzed as shown in Fig. 6c and

to different acoustic intensity levels. Statistical significance for all parameters: * $P < 0.05$; ** $P < 0.01$; *** $P < 0.001$; using one-way repeated measurement ANOVA, followed by a *post-hoc* test

f. At this time, the other elements were fixed at a level 2 acoustic intensity, a duty cycle of 50%, and a sonication duration of 20 s (Fig. 6c; spike rate: 0.73 ± 0.19 Hz at baseline, 0.8 ± 0.22 at 10 Hz, 0.86 ± 0.19 at 100 Hz, 0.78 ± 0.19 at 500 Hz, 0.95 ± 0.22 at 1 kHz, and 0.92 ± 0.22 at 2 kHz, Fig. 6f; number of bursts: 1.3 ± 0.35 at baseline, 1.43 ± 0.35 at 10 Hz, 1.47 ± 0.31 at 100 Hz, 1.4 ± 0.31 at 500 Hz, 1.81 ± 0.4 at 1 kHz and 1.76 ± 0.35 at 2 kHz). As the PRF values increased (in other words, as the stimulation cycle became more frequent), the spike rate and the burst numbers tended to rise (Fig. 6c and f).

3.4 Spontaneous neural activity in bicuculline

To identify the response of the excitatory neurons only, GABA_A receptors were blocked with bicuculline (BCC)

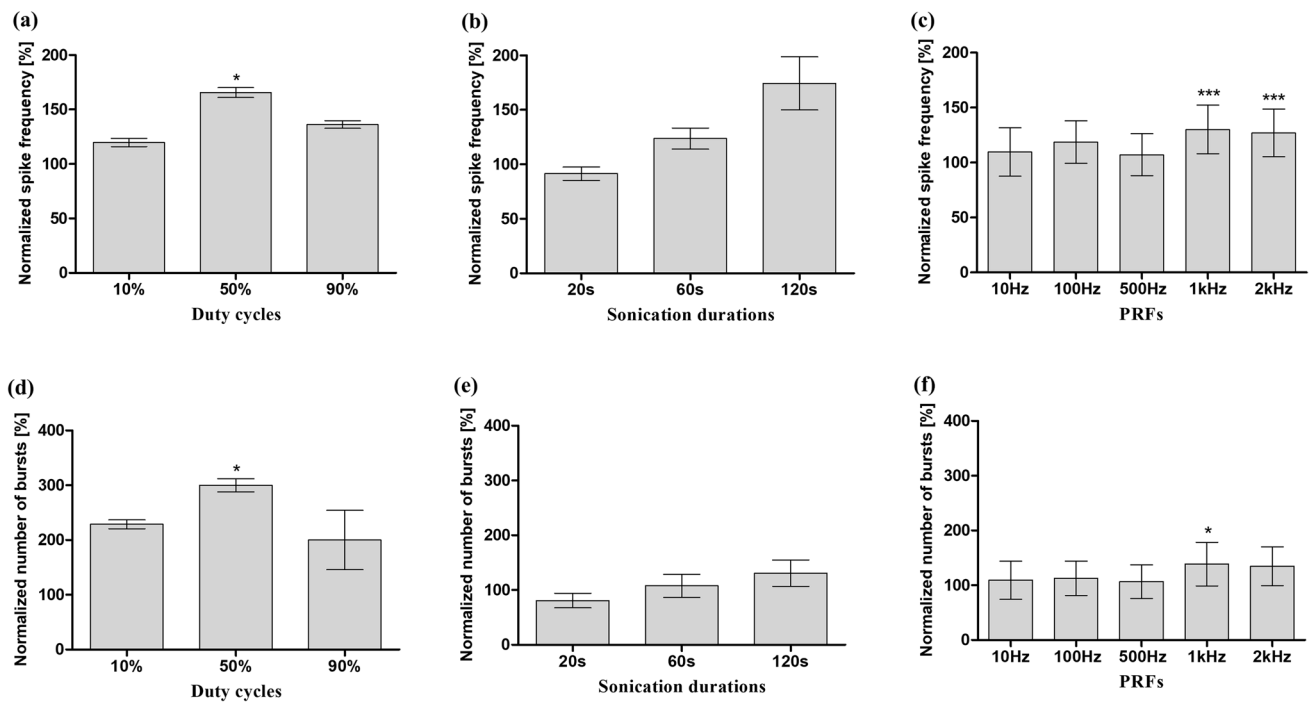


Fig. 6 Characteristics of the neuronal response (given as mean \pm SEM) to different ultrasound parameters. All graphs have been normalized to baseline. Normalized spike frequency and number of bursts in response to (a, d) different duty cycles (b, e), different

sonication durations, and (c, f) different PRFs. Statistical significance for all parameters: * $P < 0.05$; ** $P < 0.01$; *** $P < 0.001$; using one-way repeated measurement ANOVA, followed by a *post-hoc* test

that inhibits the activity of inhibitory neurons. The spike rate and the number of bursts without the bicuculline were compared with those after 1 min of treatment with bicuculline. At the presence of bicuculline, the frequency of the spikes increased more than ten times (spike rate: 0.14 ± 0.03 at without BCC and 1.94 ± 0.37 at BCC). In the case of the number of bursts was seven times higher than that without bicuculline (burst number: 0.34 ± 0.12 at without BCC and 2.61 ± 1 at BCC). These results indicate that the primary hippocampal neuronal cultures in this study include the population of inhibitory neurons as well as excitatory neurons.

3.5 Effects of bicuculline on ultrasound neuromodulation

In the presence of bicuculline, the evoked neuronal activities were analyzed for each ultrasound acoustic intensity level. The activity was assessed for one min after the ultrasonic stimulation. As the acoustic intensity increased in the raster plot in Fig. 7a, there was only a fine difference in terms of the recorded mean spike frequency. Spike frequency and number of bursts was normalized by baseline (Fig. 7b and c). When compared with baseline for each acoustic intensity level, Bonferroni *post-hoc* analysis revealed significant differences at level 1 and 5 (Fig. 7b; spike rate: 1.34 ± 0.21 at baseline, 1.53 ± 0.25 at level 1, 1.23 ± 0.19

at level 2, 1.2 ± 0.19 at level 3, 1.25 ± 0.21 at level 4, and 1.14 ± 0.18 at level 5). The spike rate increased sharply at level 1 but decreased at level 5. The number of bursts, and the mean burst duration were assessed (Fig. 7c; number of bursts: 2.17 ± 0.34 at baseline, 2.93 ± 0.5 at level 1, 2.28 ± 0.39 at level 2, 2.16 ± 0.36 at level 3, 2.02 ± 0.34 at level 4 and 1.86 ± 0.33 at level 5, Fig. 7d; burst duration: 152.2 ± 24.37 ms at baseline, 128.9 ± 23.63 ms at level 1, 140.2 ± 26.2 ms at level 2, 128.2 ± 24.79 ms at level 3, 156.8 ± 29.01 ms at level 4 and 152.8 ± 26.24 ms at level 5). When compared with baseline, the number of bursts also increased only at level 1. There was no significant difference observed in the other conditions.

The spike rates and the burst numbers were also examined for other parameters in the same way as the normal conditions without bicuculline. Figure 8a and d present the characteristics of the neuronal activities in response to different duty cycles. The frequency of the spikes and the number of bursts were normalized by baseline (Fig. 8a; spike rate: 1 ± 2.1 at baseline, 0.77 ± 0.17 at 10%, 0.96 ± 0.22 at 50%, and 0.75 ± 0.16 at 90%, Fig. 8d; number of bursts: 1.62 ± 0.38 at baseline, 1.01 ± 0.23 at 10%, 1.36 ± 0.31 at 50% and 1.33 ± 0.33 at 90%). When the duty cycles were 10% and 90%, the spike rate tended to decrease, but there was no significant difference at the 50% duty cycle. The burst number significantly decreased at 10%, whereas the

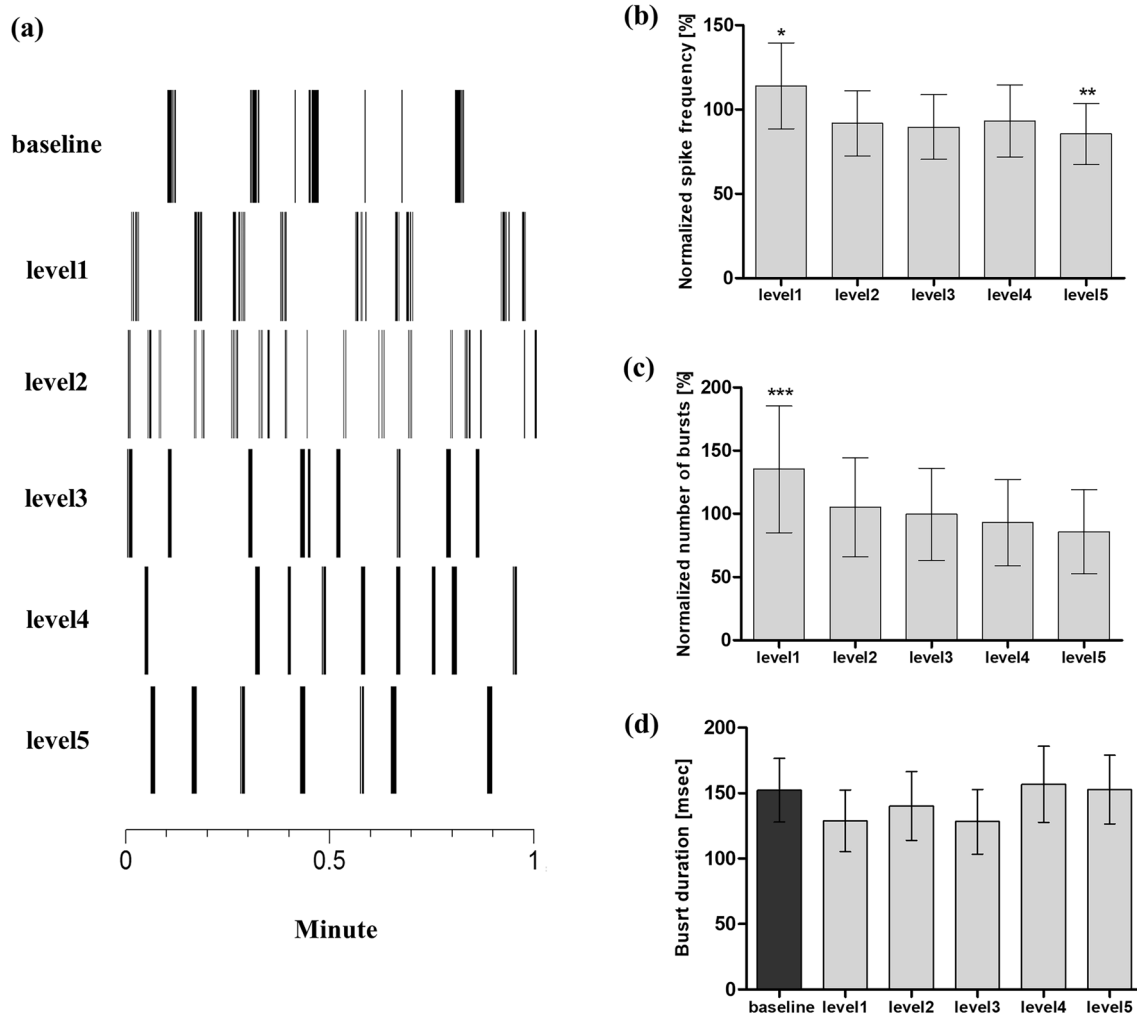


Fig. 7 Characteristics of the neuronal response (given as mean \pm SEM) to different acoustic intensity levels after a treatment with bicuculline. **a** Raster plot of neural spikes recorded on MEA. **b** Normalized spike frequency **c** Normalized number of bursts. **d**

Mean burst duration in response to different acoustic intensity levels. Statistical significance for all parameters: * $P < 0.05$; ** $P < 0.01$; *** $P < 0.001$; using one-way repeated measurement ANOVA, followed by a *post-hoc* test

others exhibited no significant differences compared to the baseline (Fig. 8d).

Figure 8b and e present the effects of the sonication duration on ultrasound neuromodulation. The frequency of the spikes and the number of bursts were normalized by baseline (Fig. 8b; spike rate: 0.91 ± 0.13 at baseline, 1.21 ± 0.18 at 20 s, 1.33 ± 0.2 at 60 s, and 1.5 ± 0.24 at 120 s, Fig. 8e; number of bursts: 2.15 ± 0.38 at baseline, 2.4 ± 0.38 at 20 s, 2.52 ± 0.39 at 60 s and 2.65 ± 0.44 at 120 s). When compared with baseline, a significant difference was identified in all sonication duration conditions assessed. As the duration of the ultrasonic waves lasted longer, the frequency of the neuronal activity increased. The number of bursts tends to be similar to the spike frequency.

The changes in the neuronal activity as a result of the application of different PRF levels were acquired (Fig. 8c;

spike rate: 0.49 ± 0.12 at baseline, 0.56 ± 0.14 at 10 Hz, 0.54 ± 0.12 at 100 Hz, 0.67 ± 0.16 at 500 Hz, 0.45 ± 0.1 at 1 kHz, and 0.52 ± 0.13 at 2 kHz, Fig. 8f; number of bursts: 1.06 ± 0.37 at baseline, 1.00 ± 0.34 at 10 Hz, 1.06 ± 0.33 at 100 Hz, 1.42 ± 0.41 at 500 Hz, 0.93 ± 0.3 at 1 kHz and 1.1 ± 0.45 at 2 kHz). As the PRF increased, no marked difference was observed, except for a rise at 500 Hz compared to the baseline.

4 Discussion

The responses of cultured hippocampal neurons to ultrasonic application were observed in terms of action potentials and bursts. We observed a noticeable increased activity in the case of applying ultrasound of the spatial-peak

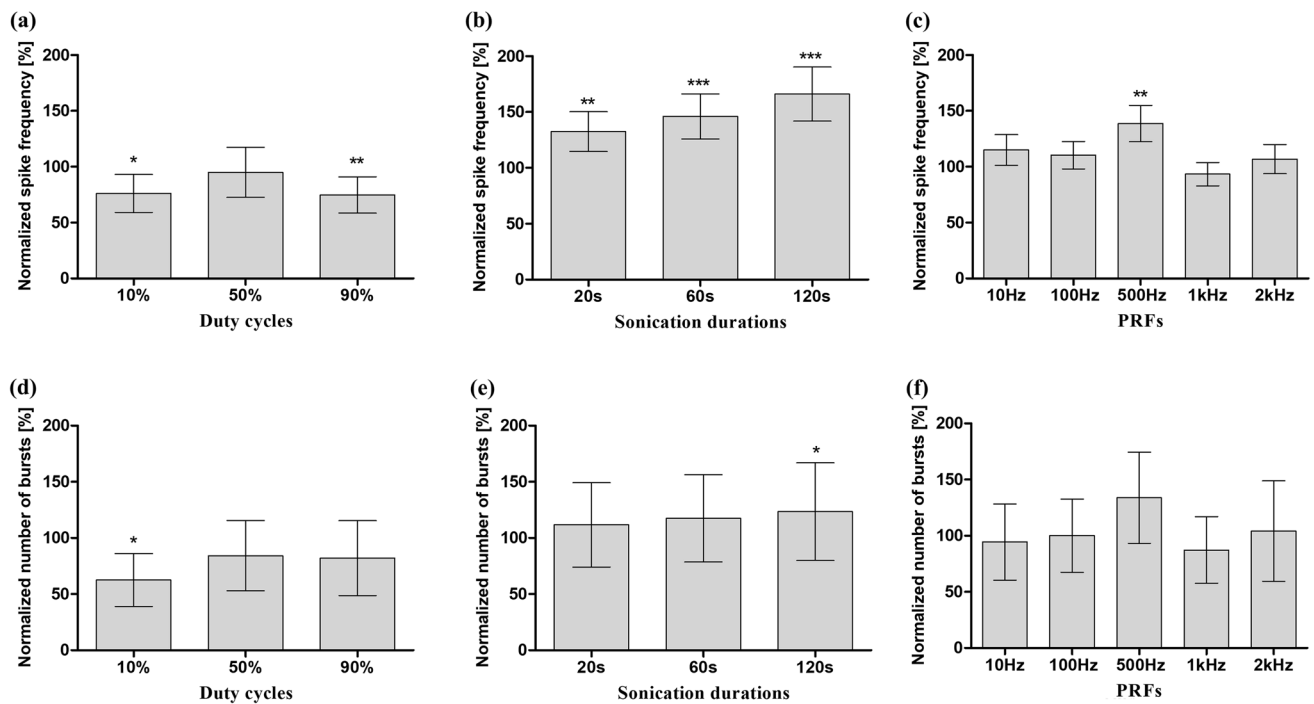


Fig. 8 Characteristics of the neuronal response (given as mean \pm SEM) to different ultrasound parameters after a treatment with bicuculline. All graphs have been normalized to baseline. Normalized spike frequency and number of bursts in response to (a, d)

different duty cycles (b, e), different sonication durations, and (c, f) different PRFs. Statistical significance for all parameters: * $P < 0.05$; ** $P < 0.01$; *** $P < 0.001$; using one-way repeated measurement ANOVA, followed by a *post-hoc* test

temporal-average intensity of 3.8 W/cm^2 with 50% duty cycle, and PRF above 1 kHz when compared with baseline. We have not identified significant differences as a result of different sonication durations, but when the irradiation time was longer, the spike rate exhibited a slight increase with an extended mean error.

Many studies have been undertaken to clarify the mechanisms of ultrasound neuromodulation, and the exact mechanism is yet to be elucidated. Our experiments have also a few agreements with the results of previous research hypotheses for thermal or mechanical activation of neurons. First, as far as the temperature is concerned, the ultrasound intensity that we used was not high enough to allow us a comparison with the HIFU. Moreover, according to most previous studies, such neuromodulation effects are not a result of a thermal reaction, and we agree with this hypothesis [26, 27]. We also observed minor temperature changes less than $0.1 \text{ }^\circ\text{C}$. If heat did not induce these activity changes, then mechanical forces or the synergistic effect of mechanical and thermal activation should be considered.

A mechanical force due to ultrasonic modulation can be explained in two ways. One is through the cavitation that occurs when media change rapidly at high speeds, in which the pressure of the media is relatively low and causes vapor bubbles in the liquid. The cavitation phenomenon can be divided into inertial and noninertial cavitation

[26]. Inertial cavitation is the process in which the formed bubbles in the media rapidly collapse. If the mechanical index exceeds 1.9 by FDA, it can be considered capable of causing inertial cavitation, which can cause cell damage. However, the experiments in this study did not exceed this MI value. Noninertial cavitation is the process in which bubbles in the fluid oscillate in size or shape in the middle of the acoustic field. According to *in vivo* experiments, noninertial cavitation led to stable bubble production when the intensity of the ultrasound was expressed between 0.1 and 3 W/cm^2 [28]. In fact, our experiments were performed within this range of ultrasonic power. Therefore, these mechanical forces might have affected the cellular activity. In order to verify if noninertial cavitation does occur under our ultrasonic application, additional experiments can be performed with degassed culture media. The other hypothesis for the induction of mechanical force is acoustic radiation as the most prominent mechanism. Ultrasonic waves can exert static pressure on a target during propagation. This steady pressure can induce a displacement of the cell states [29]. As the ultrasound waves wobble, the radiation force can oscillate mechanosensitive ion channels or other active molecules tied to the membrane directly [30]. In addition, it may cause an increase in the probability of releasing or absorbing neurotransmitter vehicles. Indirectly, the radiation force may cause a deformation of the

membrane capacitance, thereby modifying the membrane equilibrium potential [27].

In summary, our experimental results might be explained through three existing hypothetical mechanisms: first, through the hypothesis that noninertial cavitation has caused an expansion and a contraction of the bubble, followed by a displacement of the cell membrane; second, through the hypothesis that the acoustic radiation force directly oscillated the membrane to increase the probability of the channel opening; and lastly, through the hypothesis that as the radiation force raises a mismatch of the membrane capacitance, the latter indirectly leads to changes in the cell activity. These three hypothetical mechanisms may be true in our case, either individually or in combinations with each other. As some experiments were conducted within the intensity including may bring noninertial cavitation, it is thought that our research outcome will be a combined effect with the radiation force.

In addition to the mechanism of ultrasonic neuromodulation, the safety is one of the most important issues. As mentioned, the ultrasonic parameters in this study were within the safety limit of FDA in terms of mechanical index. Besides, during the experiments, no neuronal death was observed after ultrasonic exposure. However, since the nervous system is very sensitive to subtle change of environments, it is worthwhile to investigate the long-term effect of ultrasonic exposure on the viability as well as the functionality of neurons.

As far as the assessed parameters are concerned, there was experimental support that ultrasonic stimulation can be modulated in terms of both its activation and its suppression. Previous studies have suggested that bimodulation is possible through the modification of the duty cycle and the acoustic intensity [16, 30, 31]. We also observed in our experiments that the modification of the acoustic intensity parameter caused both a decrease and an increase in the APs. In terms of the duty cycle parameter, 10% is the lowest when compared with the other parameters. In another study, it was reported that the pulsed ultrasound is more efficient than a continuous wave in the *in vivo* experiment [15, 16]. In our experimental results, it tended to affect more the activity at a 50% duty cycle than at a 90% one. Therefore, we also believe that a pulse wave is more efficient for the delivery of neuromodulation than a continuous wave *in vitro*. There has been a study using a theoretical neuronal model that has suggested the possibility that a selective response from the channels would be triggered as a result of a particular duty cycle [13, 30]. This neuronal model allowed for the hypothesis that the T-type calcium channels exist in the inhibitory neurons that are activated by the low duty cycle ultrasound and ultimately suppress the total neural network activity. More specifically, this model has suggested that only inhibitory neurons were stimulated by the 5% duty cycle, and that

both excitatory and inhibitory neurons can become active when the duty cycle goes up. This theoretical model has a considerable correlation with a few previous experimental studies. However, this study has shown that a slight increase in neuronal activity can occur even at a 10% duty cycle. In the hippocampal cell cultures, excitatory neurons and inhibitory neurons are randomly placed and connected. Therefore, the result may be due to an influence of the inhibitory neurons cultured on MEA.

As described above, hippocampal cell cultures contain relatively few inhibitory neurons with the role of inhibiting the activity of the excitatory neurons at a certain ratio [32]. After suppressing the inhibitory neuron activity using bicuculline (a drug known to be used to mimic epilepsy), the same ultrasound parameter assessment experiments were performed. However, the response to ultrasound stimulation was significantly reduced with the blockage of inhibitory neurons. As a result of the experiment, the overall response to ultrasound stimulation disappeared where inhibitory neurons were blocked. Therefore, it can be assumed that the increased activity in response to ultrasound stimulation in the bicuculline-free environment is probably because the ultrasound stimulation suppressed inhibitory neurons. To verify this, it might be possible to perform an experiment in which only inhibitory neurons are cultured. However, in general, the population of excitatory neurons in the brain is much higher than the inhibitory neuron [33]. Since these ratio could be the same in culture conditions, it is difficult to make the culture conditions only with inhibitory neurons [34]. On the other hand, there is another possibility that the neuronal activity is saturated at the presence of bicuculline. This may be because either there were reached the limit of the highest neural activity or no more channels available to react.

In this study, the *in vitro* ultrasonic neuromodulation setup was established. Various parameters of the administered ultrasound were examined, and the changes of the neuronal activity were observed. Overall, the variation of the activity changes was not significant, but it demonstrated a similarity to other *in vivo* experimental results. With a 0.5-MHz center frequency ultrasound, the acoustic intensities of 7.6 W/cm² in terms of I_{SPPA} and 3.8 W/cm² in terms of I_{SPTA} , a 50% duty cycle, and a 1-kHz PRF, ultrasound neuromodulation was optimally verified. The *in vitro* experimental setup described herein could serve as a useful tool for the clarification of the mechanisms underlying the electrophysiological effects of ultrasound in further studies.

Acknowledgements We thank Prof. Tae-Seong Kim from Department of Biomedical Engineering, College of Electronics and Information, Kyung Hee University for offering ultrasound transducer and helpful comments during the writing of the manuscript. This research was supported by the National Research Foundation of Korea (NRF-2019M3C1B8090805, NRF-2022R111A4063209) and by the Korea

Medical Device Development Fund grant funded by the Korea government (the Ministry of Science and ICT, the Ministry of Trade, Industry and Energy, the Ministry of Health & Welfare, the Ministry of Food and Drug Safety) (1711139110, KMDF_PR_20210527_0006).

Author contributions Conceptualization: all authors. Methodology: HS. Investigation: HS. Writing—original draft preparation: HS. Writing—review and editing: All authors. Approval of final manuscript: all authors.

Declarations

Conflict of interest The authors have no conflicts of interest to disclose.

Ethical approval The procedures followed and the care of the animals were approved by the Institutional Animal Care and Use Committee in Ewha Womans University (Approval no. 17-010).

References

- Levy R, Deer TR, Henderson J. Intracranial neurostimulation for pain control: a review. *Pain Phys*. 2010;13(2):157–65.
- Yu X, Nagai J, Khakh BS. Improved tools to study astrocytes. *Nat Rev Neurosci*. 2020;21(3):121–38.
- Gunaydin LA, et al. Ultrafast optogenetic control. *Nat Neurosci*. 2010;13(3):387–92.
- Boyden ES, et al. Millisecond-timescale, genetically targeted optical control of neural activity. *Nat Neurosci*. 2005;8(9):1263–8.
- Eom K, et al. Synergistic combination of near-infrared irradiation and targeted gold nanoheaters for enhanced photothermal neural stimulation. *Biomed Opt Express*. 2016;7(4):1614–25.
- Tyler WJ. Noninvasive neuromodulation with ultrasound? A continuum mechanics hypothesis. *Neuroscientist*. 2010;17(1):25–36.
- George MS, Lisanby SH, Sackeim HA. Transcranial magnetic stimulation: applications in neuropsychiatry. *Arch Gen Psychiatry*. 1999;56(4):300–11.
- Nitsche MA, et al. Treatment of depression with transcranial direct current stimulation (tDCS): a review. *Exp Neurol*. 2009;219(1):14–9.
- Bystritsky A, Korb AS. A review of low-intensity transcranial focused ultrasound for clinical applications. *Curr Behav Neurosci Rep*. 2015;2(2):60–6.
- Rezayat E, Toostani IG. A review on brain stimulation using low intensity focused ultrasound. *Basic Clin Neurosci*. 2015;7(3):187–94.
- Baek H, Pahk KJ, Kim H. A review of low-intensity focused ultrasound for neuromodulation. *Biomed Eng Lett*. 2016;7(2):135–42.
- Khraiche ML, et al. Ultrasound induced increase in excitability of single neurons. *Conf Proc IEEE Eng Med Biol Soc*. 2008;2008:4246–9. <https://doi.org/10.1109/IEMBS.2008.4650147>.
- Tyler WJ, et al. Remote excitation of neuronal circuits using low-intensity, low-frequency ultrasound. *PLoS ONE*. 2008;3(10):e3511.
- Muratore, R. et al.: Bioeffects of low dose ultrasound on neuronal cell function. In 2009 38th Annual Symposium of the Ultrasonic Industry Association (UIA). 2009.
- Tufail Y, et al. Ultrasonic neuromodulation by brain stimulation with transcranial ultrasound. *Nat Protoc*. 2011;6(9):1453–70.
- Kim H, et al. Focused ultrasound-mediated non-invasive brain stimulation: examination of sonication parameters. *Brain Stimul*. 2014;7(5):748–56.
- Lee W, et al. Creation of various skin sensations using pulsed focused ultrasound: Evidence for functional neuromodulation. *Int J Imag Syst Technol*. 2014;24(2):167–74.
- Beaudoin GM 3rd, et al. Culturing pyramidal neurons from the early postnatal mouse hippocampus and cortex. *Nat Protoc*. 2012;7(9):1741–54.
- Yao J, Qi J, Chen G. Actin-dependent activation of presynaptic silent synapses contributes to long-term synaptic plasticity in developing hippocampal neurons. *J Neurosci*. 2006;26(31):8137–47.
- Li X, et al. Long-term recording on multi-electrode array reveals degraded inhibitory connection in neuronal network development. *Biosens Bioelectron*. 2007;22(7):1538–43.
- Geissler M, Faissner A. A new indirect co-culture set up of mouse hippocampal neurons and cortical astrocytes on microelectrode arrays. *J Neurosci Methods*. 2012;204(2):262–72.
- Xiang G, et al. Microelectrode array-based system for neuropharmacological applications with cortical neurons cultured in vitro. *Biosens Bioelectron*. 2007;22(11):2478–84.
- Ahn S, et al. Study on the mechanisms of seizure-like events suppression effect by electrical stimulation using a microelectrode array. *NeuroReport*. 2017;28(9):471–8.
- Gross GW, et al. The use of neuronal networks on multielectrode arrays as biosensors. *Biosens Bioelectron*. 1995;10(6–7):553–67.
- Hochman DW, et al. Extracellular chloride and the maintenance of spontaneous epileptiform activity in rat hippocampal slices. *J Neurophysiol*. 1999;81(1):49–59.
- King RL, et al. Effective parameters for ultrasound-induced in vivo neurostimulation. *Ultrasound Med Biol*. 2013;39(2):312–31.
- Tyler WJ, Lani SW, Hwang GM. Ultrasonic modulation of neural circuit activity. *Curr Opin Neurobiol*. 2018;50:222–31.
- ter Haar G. Therapeutic applications of ultrasound. *Prog Biophys Mol Biol*. 2007;93(1–3):111–29.
- Kubanek J. Neuromodulation with transcranial focused ultrasound. *Neurosurg Focus*. 2018;44(2):E14–E14.
- Kubanek J, et al. Ultrasound elicits behavioral responses through mechanical effects on neurons and ion channels in a simple nervous system. *J Neurosci*. 2018;588:4969.
- Plaksin M, Kimmel E, Shoham S. Cell-type-selective effects of intramembrane cavitation as a unifying theoretical framework for ultrasonic neuromodulation. *eneuro*. 2016;3:ENEURO.0136-15.2016.
- Wu YK, Fujishima K, Kengaku M. Differentiation of apical and basal dendrites in pyramidal cells and granule cells in dissociated hippocampal cultures. *PLoS ONE*. 2015;10(2):e0118482.
- Alreja A, Nemenman I, Rozell CJ. Constrained brain volume in an efficient coding model explains the fraction of excitatory and inhibitory neurons in sensory cortices. *PLoS Comput Biol*. 2022;18(1):e1009642.
- Xu J-C, et al. Cultured networks of excitatory projection neurons and inhibitory interneurons for studying human cortical neurotoxicity. *Sci Transl Med*. 2016;8(333):33348–33348.

Publisher's Note Springer Nature remains neutral with regard to jurisdictional claims in published maps and institutional affiliations.

Springer Nature or its licensor (e.g. a society or other partner) holds exclusive rights to this article under a publishing agreement with the author(s) or other rightsholder(s); author self-archiving of the accepted manuscript version of this article is solely governed by the terms of such publishing agreement and applicable law.